



## ORIGINAL RESEARCH PAPER

## Photochemical oxidation and landfarming as remediation techniques for oil-contaminated soil

M. Mambwe<sup>1</sup>, K.K. Kalebaila<sup>1\*</sup>, T. Johnson<sup>2</sup><sup>1</sup> Department of Chemistry, School of Mathematics and Natural Sciences, Copperbelt University, Kitwe, Zambia<sup>2</sup> Department of Biological Sciences, School of Mathematics and Natural Sciences, Copperbelt University, Kitwe, Zambia

## ARTICLE INFO

**Article History:**

Received 18 October 2023

Revised 22 November 2023

Accepted 2 January 2024

**Keywords:**

Degradation

First-order kinetics

Half-life

Landfarming

Modified clays

Photochemical oxidation

## ABSTRACT

**BACKGROUND AND OBJECTIVES:** With technological advances, mining industries use more crude oil and its products. Finding fast, effective, and eco-friendly repair techniques for oil-contaminated soil is crucial. Clay–titanium dioxide/manganese was used to investigate how oil breaks down in soil under sunlight. Various soil remediation techniques have been used to discard oil pollutants in soil. A polluted site must be cleaned effectively with a suitable method. Natural attenuation takes too long to produce positive results, whereas landfarming can produce toxic intermediates due to the organisms' inability to degrade other oil components. Photochemical oxidation is a promising eco-friendly technique that can be employed as an alternative remediation method. The speed at which natural attenuation, photochemical oxidation, and landfarming could remove oil from contaminated soils was examined. Photochemical oxidation's superiority as a remediation technique over landfarming is hypothesized.

**METHODS:** Using clay modified with titanium dioxide and manganese, the effectiveness of landfarming and photochemical oxidation on oil-contaminated soil was investigated, together with the processes' kinetics. To establish the processes' effectiveness and kinetics, the oil residue was calculated at 7-day intervals for 35 days.

**FINDINGS:** Initial oil concentration was 56.6 milligrams per kilogram, and degradation rates ranged from 23.91-80.47 percent. Highest oil reduction was 10.86 milligrams per kilogram. Combined remediation (biocarb and grafted clays) produced high degradation rate constants,  $k$  (0.046-0.049/day) and low degradation half-lives,  $t_{1/2}$  (15.2, 17.4 days). Photochemical oxidation rate constants ranged from 0.015-0.03984/day and half-lives ranged from 17.395-44.971 days, whereas landfarming had a rate constant of 0.008 and half-life of 83.094. Natural attenuation had the lowest  $k$  (0.007) and longest half-life ( $t_{1/2}$ ) of 94.8 days. Significant differences in means were observed among treatments (control, biocarb, and bicarb + grafted clays) at  $p \leq 0.05$ , suggesting that treatment caused oil decrease in microcosms for biocarb + grafted clays. Grafted clays plus biocarb show potential for combined remediation of oil-contaminated soil.

**CONCLUSION:** One primary indicator used to assess treatments' efficacy is oil reduction, calculated using difference in oil content in soil before and after remediation. This shows that oil can be quickly removed from oil-contaminated soil by using biocarb + grafted South Luangwa with 80 percent oil reduction. Results suggest that photochemical oxidation may be used to effectively degrade oil and shorten remediation time. Photochemical oxidation is environmentally friendly and degrades oil faster than landfarming. Zambia's Mopani Copper Mines can consider adopting photochemical oxidation as a remediation technique in treating oil-contaminated soil.

DOI: [10.22035/gjesm.2024.02.07](https://doi.org/10.22035/gjesm.2024.02.07)This is an open access article under the CC BY license (<http://creativecommons.org/licenses/by/4.0/>).

NUMBER OF REFERENCES

92



NUMBER OF FIGURES

7



NUMBER OF TABLES

6

\*Corresponding Author:

Email: [kkalebai@gmail.com](mailto:kkalebai@gmail.com)

Phone: +2609 6452 5969

ORCID: [0000-0003-3561-841X](https://orcid.org/0000-0003-3561-841X)

Note: Discussion period for this manuscript open until July 1, 2024 on GJESM website at the "Show Article".

## INTRODUCTION

The entire world relies on crude oil as a clean energy source, which ultimately encourages widespread exploration, refining, transportation, and consumption of crude oil-derived goods (Khudur et al., 2015; Sharifi, 2022). As one of the primary sources of fuel, crude oil continues to have an impact on numerous nations. The degree to which life has become easier in contemporary communities because of the oil, which is simple to use and locate, cannot be overemphasized. However, it is impossible to overlook the pollution it causes, particularly soil degradation when used in sectors such as mining, transportation, and the oil and gas industry. Alkanes or paraffins with 1 to 40 carbon (C) atoms per molecule make up the majority of oil wastes, whereas some crude oil may also contain significant amounts of polyaromatic hydrocarbons (PAHs) (Imam et al., 2019). PAHs tend to adsorb on solid particles due to their hydrophobic and recalcitrant properties, which makes them one of the main soil contaminants (Thacharodi et al., 2023). These oil wastes are produced by the petroleum industry, auto repair shops, oil cleaning facilities, and other industries. To reduce harmful environmental consequences and the risk to human health posed by oil wastes, which can become pollutants in soil, sediment, and water, extensive efforts are being made to remediate them (Kebede et al., 2021; Samimi and Shahriari Moghadam, 2020). The United States Environmental Protection Agency (USPA) classifies them as priority environmental contaminants due to their toxicity, mutagenic and carcinogenic properties, as well as their persistence in the environment, which may have an impact on human health and the ecosystem (Michael-Igolima et al., 2022). Soil contamination from crude oil and petroleum products is now a serious problem for the environment because of the potential consequences for the ecosystem and human health (Naeem and Qazi, 2020). Spilt oil and waste products from the petrochemical and petroleum sectors are major sources of environmental pollution that have affected local ecosystems and their inhabitants. This oil can have persistent sub-acute toxicological effects, which can change population dynamics and disturb trophic relationships and the structure of natural communities within ecosystems (lower growth and reproduction, poor health, low recruitment rates, etc.) (Aichner et al., 2013). The immediate repercussions of these oil spills include the death of animals and plants and the

disruption of food chains and ecology. The long-term effects include birth abnormalities and genetic changes (Akinwumiju et al., 2020). Even though crude oil is not categorized as a hazardous chemical, it is nonetheless regarded as persistent due to its derivatives, which have the potential to bioconcentrate and bioaccumulate in food chains (Shaker and Almkhtar, 2016). The introduction of crude oil into the ecosystem has affected the health of people, plants, and animals because the majority of its elements are carcinogenic and cause more than 0.005 billion deaths annually (Idowu et al., 2019). Oil pollution has terrible consequences on the soil because it changes the microbial population, the structure and content of organic matter in the soil, and the enzymatic activities that take place there (Yang et al., 2017). This hinders plant growth and development. Waste oil contaminates surface and groundwater systems by adhering to soil components and is typically difficult to remove or degrade (Michael-Igolima et al., 2022). The presence of crude oil in the soil causes the environment to become anaerobic by obstructing the flow of air, which has an impact on the microbial populations in the soil (Sutton et al., 2013). When crude oil spills on land, it limits water absorption by making the soil hydrophobic—it repels water—and when it falls on grass and agricultural fields, it often kills plant life (Brown et al., 2017). Oil spills generate an imbalance in the carbon–nitrogen (C–N) ratio at the spill site because crude oil is mostly made of carbon and hydrogen. This results in phosphorus and nitrogen deficiency in oil-soaked soil, which slows down bacterial growth and carbon source utilization(s) (Agarry et al., 2013; Samimi and Shahriari-Moghadam, 2021). The components of crude oil break down at varying rates, with the heavier compounds such as cycloalkane being more resistant to microbial attack in the soil, whereas the lighter hydrocarbons break down quickly even under abiotic conditions (Abioye et al., 2011). If not removed, spilt crude oil could be retained in soil cavities and build up a significant bank of residual saturation, which could lead to significant groundwater contamination (Dzionek et al., 2016). Additionally, the potential of hydrogen (pH) and total organic carbon (TOC) content of the soil might change when crude oil is added to it (Okoh et al., 2020). The pH varies greatly across a large range and affects solubility in the soil, which therefore affects the availability of different soil elements. When the pH is close to 8, the level of bacterial activity in the

soil is improved. The remaining bulk of crude oil becomes denser and less mobile as a result of volatilization and solubilization. As part of the organic matter in the soil, the partially decomposed hydrocarbon is absorbed, creating an asphalt crust that is more difficult to biodegrade (Brown *et al.*, 2017). Finding low-cost environmental clean-up methods to decrease, degrade, or remove the pollutants has become necessary due to the scale of environmental pollution caused by crude oil-related operations. The development of soil remediation methods has received a lot of attention, and several novel and creative approaches to the effective removal of contaminants from soils have been explored to bring the contaminant's contents down to a level that is safe and acceptable (He *et al.*, 2014; Silva-Castro *et al.*, 2013). Landfarming and photochemical oxidation are some of the techniques used in oil remediation (Saneha *et al.*, 2023). In land farming, conventional farming techniques including tilling, bulking (which improves soil uniformity for biodegradation and aeration), irrigation (which supplies moisture), and fertilizer application (Samimi *et al.*, 2023) (provides nutrients to enhance the population of oil degraders) are used. Aspects that restrict its degradation efficiency, including the low number of oil degraders, superficial treatment as 10-35 centimeters (cm) of soil layer, poor contaminant uptake, and low bioavailability offset its unique benefit of promoting the natural bacteria (Sakshi and Haritash, 2019). Because landfarming is an ex-situ remediation method, the contamination is moved to another area for treatment after procedures take place off-site. As a result, unlike other remediation approaches such as photochemical oxidation, which may be done in-situ, it becomes more expensive with increased human participation and direct contact to toxins. Also, because it employs natural microbes to degrade oil, the technique is not always successful because some of them (microbes) cannot degrade some components of oil (Kong *et al.*, 2018). Photochemical oxidation, in contrast, is a process of transforming a chemical compound using sunlight (Hadnadjev-Kostic *et al.*, 2014). Ultraviolet or light technique (UV or sunlight) is applied to a mixture of the contaminant and a catalyst, causing the organic pollutants to oxidize and create compounds such as carbon dioxide and water. Semiconductor catalysts consist of an empty conduction band with higher energy and a valence band containing electrons ( $e^-$ )

that are energetically stable. Exposure of these semiconductors to light triggers photocatalytic reactions by promoting an  $e^-$  into the conduction band and creating a hole ( $h^+$ ) in the valence band (Liu and Zhang, 2014). As a result, hydroxyl ( $OH^\bullet$ ) and superoxide ( $O_2^\bullet$ ) anion radicals are produced through photocatalytic reactions, leading to the photochemical oxidation of oil at the semiconductor surface. Because photochemical oxidation may be performed in situ, unlike landfarming, which typically requires transferring the contaminated soil from one location to be treated in another, it has the potential to be used in big field undertakings. As a result, there is less chance of contamination, less expense, and less human interaction (Kong *et al.*, 2018). According to earlier findings, photooxidation can eliminate all forms of oil-related molecules, indicating that oil constituents can be removed nonselectively (Brame *et al.*, 2013). Removing oil deposits without causing environmental contamination is possible with the use of titanium dioxide ( $TiO_2$ )/clay composite. In the process of decomposing oil and other organic pollutants in the soil, this remediation strategy is not adequately used (Wang *et al.*, 2014). The use of modified Zambian clay materials in the remediation of oil-contaminated soil has not been studied. Some components of oil are known to be persistent and recalcitrant, meaning they might not be degraded by organisms in the soil. As such, the goal of this study was to assess the feasibility of photochemical oxidation using clay materials modified with a nontoxic transition metal and biodegradable silanes in the remediation of oil-contaminated soil.  $OH^\bullet$  radicals generated during light illumination are nonselective and therefore can degrade all forms of oil constituents. The primary aim of this study was to determine an alternative or supplement to the landfarming strategy now employed by one of Zambia's biggest copper mines. In particular, a less expensive and speedier method of remediating oil-contaminated soil was sought. It was found that photochemical oxidation was more effective than landfarming in oil degradation. Both landfarming and photochemical oxidation treatment have advantages in that they have a low impact on the environment and are energy efficient, with straightforward technology design and implementation. The current study was carried out at the Copperbelt University and Mopani Copper Mines (MCM), Zambia in 2023.

Table 1: Oxide composition, surface area, and pore volume of the clays

Clay	SiO <sub>2</sub>	Al <sub>2</sub> O <sub>3</sub>	Surface area (m <sup>2</sup> /g)	Pore volume (cm <sup>3</sup> /g)
UC	52.41	13.89	16.78	0.043
MC	-	-	17.98	0.048
UL	35.08	13.85	50.70	0.059
ML	-	-	64.51	0.068



Fig. 1: MCM spillsorb farm

## MATERIALS AND METHODS

### Clay additives characterization

The clay samples (both modified and unmodified) were characterized by X-ray fluorescence (XRF), inductively coupled plasma (ICP), Brunauer-Emmett-Teller (BET), and Barret-Joyner-Halenda (BJH). From previous studies, the following properties were determined for the various raw and engineered clay materials used in this study. Table 1 shows a summary of the results previously obtained for the unmodified and modified clays. Elemental composition by XRF and ICP showed that unmodified South Luangwa (UL) had a 2.5 silicon dioxide: aluminum oxide (SiO<sub>2</sub>: Al<sub>2</sub>O<sub>3</sub>) ratio, and 3.8 for unmodified Chingola (UC). The surface area and pore sizes were higher in modified South Luangwa (ML) at 64.5081 square meter per gram (m<sup>2</sup>/g) and 0.068 nanometer (nm) compared to modified Chingola (MC) at 17.9780 m<sup>2</sup>/g and pore volume at 0.048 cubic centimeter per gram (cm<sup>3</sup>/g). Both fourier transform infrared (FTIR) spectra showed and confirmed the presence of grafted hydrophobic silanes, whereas the ultra violet-visible spectroscopy (UV-Vis) confirmed the incorporation of manganese (Mn) because a red shift in energy was observed in both ML at 3.1 e<sup>-</sup> (eV) and MC at 2.5 eV (Mambwe et al., 2023).

### Soil sample collection

Oil-contaminated soil samples were collected from the MCM spillsorb farm (Fig. 1) situated approximately 11 kilometers (km) southeast of Kitwe, Copperbelt Province, Zambia with latitude 12° 48' 13.79"S and longitude 28° 12' 47.30"E. The study area is located in an isolated area where the temperature ranges from approximately 20 degrees Celsius (°C) to 50 °C for purposes of soil remediation. Random sampling was employed during the collection of contaminated soil samples. The samples were collected in a zig-zag pattern across the field. The representative laboratory-size sample was achieved by the quartering method, and the process was repeated several times to ensure proper mixing of the soil. About 10 kilograms (kg) of contaminated soil were collected, and the soil was removed within the band wall from the top of the heap of soil using a shovel and placed in polythene bags, which were later transported to the chemistry laboratory at the Copperbelt University for sample treatment.

### Contaminated soil sample preparation

The first step in soil preparation was to let the soil dry naturally for a few days without exposing it to



Fig. 2: Oil-contaminated soil samples

direct sunshine in a clean, well-ventilated laboratory. To speed up the drying process, the aggregated soils were crushed. The soils were cleared of disturbing elements including stones, leaves, and bits of wood. After being dried, the soils were poured through 2 millimeter (mm) sieves. The soils that were retained were crushed once again and sieved. Then, the soils were homogenized by mixing them until oils were assumed to have the same concentration within the soils (Effendi and Aminati, 2019). The prepared samples are shown in Fig. 2.

#### Soil characterization

To understand how the physical and chemical characteristics of contaminated soil affect the pace of oil breakdown, temperature, moisture content, and pH were determined (Okoh *et al.*, 2020). To determine the pH, 10 grams (g) of air-dried soil was obtained for the test, and 10 milliliter (mL) of reagent water was added and mixed. A pH electrode was then used to measure the supernatant (Lin *et al.*, 2022). The dry-wet method was used to calculate the moisture content (Okoh *et al.*, 2020). The procedure of dry wet involves drying the soil sample and calculating the weight difference between the wet and dry samples to determine the moisture content directly.

#### Determination of the initial amount of oil in the contaminated soil sample

The solvent extraction method was used to

gravimetrically measure the amount of oil present in the contaminated soil sample. A 50 mL flask containing around 10 g of the contaminated soil sample was filled with 20 mL of n-hexane. To allow the hexane to extract the oil from the soil sample, the mixture was violently agitated on a magnetic stirrer for 30 minutes (min). A Whatman filter paper was used to filter the solution, and the liquid phase extract (filtrate) was then diluted by adding 1 mL of the extract to 50 mL of hexane (Almutairi, 2022). During the treatment process, oil content was analyzed with the use of total oil grease/total petroleum hydrocarbon (TOG/TPH) infracal. Ten grams (10 g) of clumpy, damp soil samples were mixed with 5 g of sodium sulphate to prevent water from interfering with the analysis. An extraction ratio of 1:2 was achieved by adding twice the extraction solvent (Horiba S-316) as the soil sample weight. After that, the samples were left on the mechanical shaker for an hour. A Whatman filter paper was used to filter the solvent, which included about 1 g of silica gel, and the solvent was then transferred into a sterile beaker (silica gel is used for the removal of polar organics before TPH analysis) (Fanaei *et al.*, 2020). Using measurements taken, Eq. 1 was applied to calculate the percentage decrease in total oil content (Soliman *et al.*, 2014; Samimi and Safari, 2022).

$$\%R = \frac{(C_o - C_e)}{C_o} \times 100 \quad (1)$$

where  $C_o$  is the initial amount of oil in the soil (at

time of 0),  $C_e$  is the amount of oil in the soil at time (t), and percent (%)R is the percentage of oil degradation after treatment (Farooq et al., 2022; Hussain et al., 2017).

#### Determination of total organic carbon

Using the modified wet combustion method, TOC was calculated. The Walkley and Black wet combustion method was used to calculate TOC (Jha et al., 2014). In this procedure, a 250 mL Erlenmeyer conical flask was filled with a 1 g contaminated soil sample. After that, 10 mL of a 0.16 Molar (M) potassium dichromate solution was added to the flask's contents, and the flask was gently shaken to ensure that the contents were thoroughly mixed. The contents of the flask were gently mixed with 20 mL of concentrated sulphuric acid before being left to stand for 5 min under a fume hood. The contents of the flask were then filled with distilled water until the total volume was around 125 mL, and the flask was gently spun. After 30 min, the flask's contents were allowed to cool to room temperature (the addition of sulphuric acid warms the mixture). Thereafter, 1.0 M ferrous sulphate solution was used to titrate the mixture before adding 5 or 6 drops of phenanthroline complex. The color of the solution changed from green to reddish-brown as the titration's endpoint was reached. The same process was used for a blank titration, but without a sample (Jha et al., 2014).

#### Statistical analysis

A one-way analysis of variance (ANOVA) test was used to compare means of the oil removal treatments performed. A Fisher's least significant difference (LSD) multiple comparison test was also conducted using Statistical Package for Social Sciences (SPSS) software (Sanie Jahromi et al., 2023) version 27 at 95% confidence interval. Fig. 6 was plotted using OriginPro software version 2021. The bar charts (Figs. 4 and 5) were plotted in Microsoft Excel and SPSS respectively. The coefficient of determination ( $R^2$ ) was used to measure how well the data fit into the statistical model (first-order kinetics model) used in the study.

#### Treatment of oil-contaminated soil samples

Contaminated soil samples (500 g) were put into 8 different plastic basins (microcosms), and each basin was labeled. The contaminated soil samples were treated with modified clay samples, namely

UC and UL. These clay samples were modified by incorporation of  $TiO_2$  and Mn ions, and then part of the modified samples was further modified by grafting with isobutyltrimethoxysilane to improve their photocatalytic and adsorption properties respectively. Briefly, a beaker filled with 300 mL of ethanol was filled with a 50 g sample of each clay (UC and UL). The samples were weighed and spread to create a slurry, which was left suspended for a full day before being mixed. For 15 min, the slurry was continuously stirred while 10.25 mL of acetylacetone, a complexing agent, was added. One gram (1 g) of manganese (II) nitrate ( $Mn(NO_3)_2$ ) was added, while 16.7 mL of titanium isopropoxide ( $Ti(OPr_4)$ ) was also subsequently added to the reaction mixture. After that, the mixtures were dried for 6 hours at 80 °C in the oven, and then the materials were crushed and calcined for 3 hours at 550 °C. In this study, these clays are referred to as MC and modified UL. Ten grams (10 g) of the modified and calcined clay (MC and ML) were later grafted with 10.75 mL of isobutyltrimethoxysilane, which was added dropwise under constant stirring for 24 hours after being dispersed in ethanol: water mixture (4:1, volume per volume) (v:v) in a round bottom flask at room temperature. The mixture was then allowed to react for 3 hours at 110 °C. After filtering, the mixture was cleaned of the unreacted silanes using toluene. Following surface modification, the clays were dried for 4 hours at 50 °C in an oven. These clays were then referred to as grafted Chingola (GC) and grafted South Luangwa (GL) (Mambwe et al., 2023). The prepared contaminated soil samples are shown in Fig. 2. Four different forms of treatment were used, and the water content was kept between 20% and 50% of its water-holding capability (Sihag et al., 2014). The treatments are depicted in Fig. 3 and are explained by the following steps:

#### 1- Natural attenuation

This utilized the natural ability of the soil to break down pollutants. No additives were added, and it served as a control.

#### 2- Landfarming

The experiment under landfarming conditions was done to mimic the treatment method at MCM spillsorb farm where the contaminated soil samples were obtained. In this method, biocarb (B) (nutrients) were included to promote organic biodegradation.

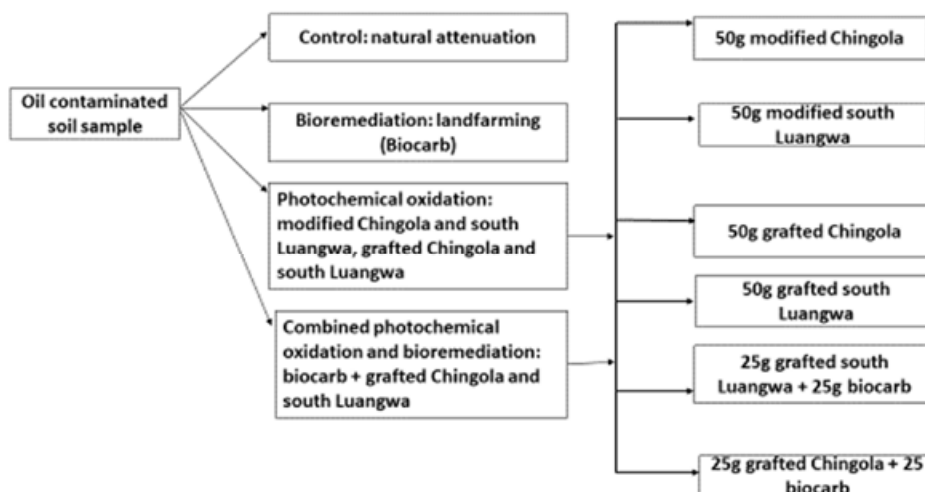


Fig. 3: Contaminated soil sample treatment setup (Effendi and Aminati, 2019)

Table 2: Moisture content and pH values of oil-contaminated soil samples after treatment

Sample	Moisture content (%)	pH values
Control	28.02	5.5
Biocarb	30.84	5.7
MC	35.06	5.8
GC	36.95	6.1
ML	35.73	5.9
GL	38.64	6.6
B+ GC	43.30	6.8
B+ GL	45.58	7.6

Thus, this treatment sample was labeled biocarb.

### 3- Photochemical oxidation

Modified and grafted clay samples (Chingola and South Luangwa) were added as photocatalysts to aid in the degradation of oil in the soil. The microcosms were labeled according to the method of modification, that is, MC, ML; modified with TiO<sub>2</sub>/Mn, GC and GL (modified clay samples grafted with isobutyltrimethoxysilane).

### 4- Combined landfarming and photochemical oxidation

Using a combination of biocarb and modified and grafted clay photocatalysts, the treatments were labeled B + GC and B + GL. The amounts of each photocatalyst added to the contaminated soil are shown in Fig. 3. The ratios were adapted from Okonofua et al. (2020) and Effendi and Aminati (2019).

All the treatments were subjected to the same controlled conditions in the greenhouse, but they were exposed to sunlight on sunny days. For aeration, each basin's contents were tilled twice a week, and the

moisture level was kept at 20-50% by adding water. The frequency of tilling was helpful in improving light penetration (Hadei et al., 2021). For 35 days, 7-day interval sampling from each plastic basin was done to determine how much oil was still present.

## RESULTS AND DISCUSSION

### Temperature

The physical and chemical parameters of temperature, moisture, and pH were determined because they have an impact on photochemical oxidation and landfarming. The rate of photochemical oxidation is increased by a high temperature caused by a high irradiation intensity (Hadei et al., 2021). The experiments were carried out at temperatures in the range of 25-40 °C, with the ideal temperature being around 40 °C on sunny days. In photochemical oxidation, e<sup>-</sup>-hole creation predominates in conditions of higher light intensity, and e<sup>-</sup>-hole recombination is minimal, leading to increased degradation of the

### Remediation of oil-contaminated soil

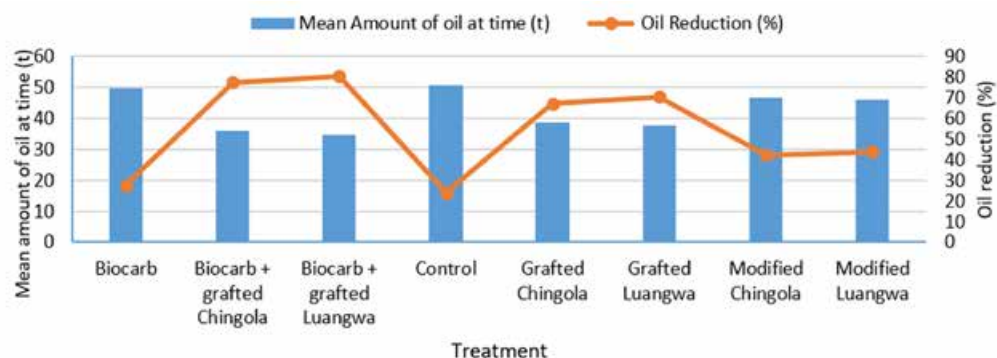


Fig. 4: Trends in oil degradation with time

pollutants (Gu *et al.*, 2012). Likewise, in landfarming, a high temperature of about 40 °C leads to increased degradation (Hesnawi and Mogadami, 2013). At very high temperatures (above 40 °C), many bacterial species experience a decline in vigor as a result of damage to their cellular structures, leading to reduced biodegradation (Stepanova *et al.*, 2022). Temperature has a considerable effect on the ability of the in-situ microorganisms to degrade oil. The solubility of oil increases with temperature, which ultimately increases the bioavailability of the oil molecules (Sihag, *et al.*, 2014).

#### Moisture

In both photochemical oxidation and landfarming, soil moisture is necessary because it promotes OH<sup>\*</sup> radical production and microbial activity, which significantly impact the method's effectiveness. The ideal moisture range, which permits oxygen to get through for microbial respiration, will allow for a soil moisture level between 20 and 50 percent of its water-holding capacity (Okoh, *et al.*, 2020). All the contaminated soil samples used in this work had moisture content greater than 20% as required (Table 1). If contaminated soil is saturated with water, oxygen will not be able to move through it. The presence of a proper amount of water can facilitate degradation, mostly because water creates favorable conditions for delivering pollutants to the catalyst surface. Because water is required for the production of OH<sup>\*</sup> in photochemical oxidation, the oil removal process increases with rising humidity (Mekkiyah *et al.*, 2023).

#### pH

The pH of the oil-contaminated soil samples (control

samples) collected from MCM before treatment was 4.5. The low pH of the oil-contaminated soil samples may be due to the presence of several free cations in the oil, which gives them the characteristics of a weak acid (Akpoveta *et al.*, 2011). A considerable increase in pH (from 5.5-7.6) was seen in microcosms after treatment (Table 2), suggesting a reduction in the oil content of the soil (Akpoveta *et al.*, 2011).

#### Total oil reduction analysis

Samples from the experimental and control groups were collected on days 0, 7, 14, 21, 28, and 35 to analyze the total oil content and kinetics of oil deterioration (Mohajeri *et al.*, 2013). The oil concentration at day 0 in the oil-contaminated soil was 56.6 mg/kg as determined by the TOG/TPH infracal method. Fig. 4 shows the trends in the oil reduction in the experimental and control setups. The table shows the amount of oil still present in the soil at a specified time in days.

The oil reduction was more in the biocarb + grafted South Luangwa (80.47%), whereas the least oil reduction was seen in the control (23.91%). The percentage of oil reduction in the control was comparable with the residue in the biocarb. The outcomes of the present investigation are in agreement with the findings of Wu *et al.* (2017) and Sarkar *et al.* (2005). When compared to natural attenuation, the addition of nutrients to the oil-contaminated soil in both studies did not improve the oil removal. In an earlier study by Wang *et al.* (2016), it was found that after 175 days of landfarming with fertilizer addition in the microcosm, a TPH elimination efficiency of just 37% was reached in an aged lubricant and diesel-oil polluted field soil. The nature and concentration of

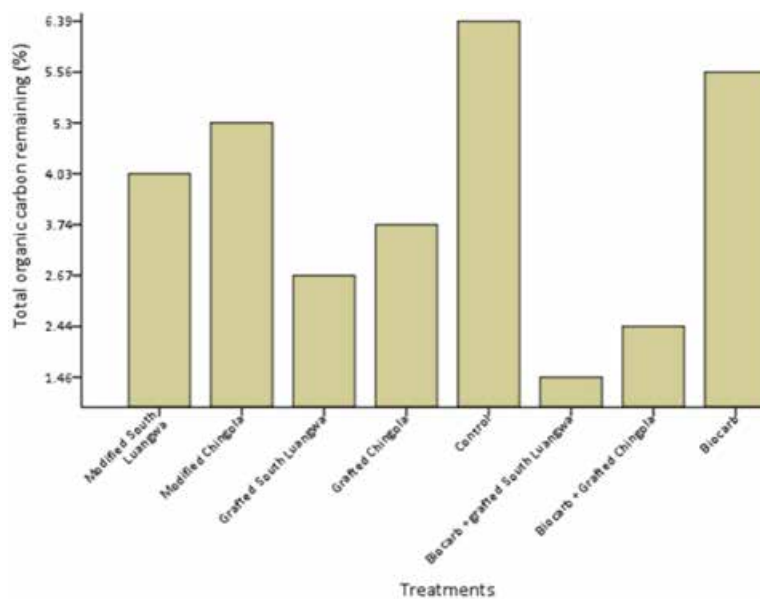


Fig. 5: Relative amount of organic carbon remaining in each soil sample

oil contamination may also be considerably impacted by physical and chemical weathering, which makes it more challenging for natural biodegraders to function. Moreover, the complex mixes of these oils that are meant to be available and accessible may contain substrates that are too large for the native microbial communities to break down (Yuniati, 2018). PAHs are among the components of crude oil that are particularly concerning because they are likely carcinogens and persist in the environment due to being resistant to microbial breakdown (Kang *et al.*, 2020). Poor solubility in soil aqueous solution and the oil absorbed on soil particles may result in poor bioavailability. This retards the biodegradation rate of the oil at the solid–liquid interface of the soil (Zhang *et al.*, 2020). That said, the higher reduction in biocarb + grafted South Luangwa could be attributed to a number of factors including high surface area, the presence of interlayer cations, as well as adsorption, which leads to the accumulation and delivery of the oil pollutants onto the clay surface, enhancing the degradation of the oil (Ugochukwu *et al.*, 2014). The relatively higher ratios of silicon per aluminum (Si/Al) in the current study indicate that the clays have high porosity (Schackow *et al.*, 2020). A high porosity facilitates the easy transit of the pollutants and degradation products inside the porous framework of the clay catalyst. This is because, according to Dlamini *et al.* (2022),  $\text{TiO}_2/\text{clay}$  photocatalysts degrade

pollutants by the adsorb-degrade-release kind of mechanism. The higher ratios also provide information on the material's permeability against humidity (Baloyi *et al.*, 2018). Good permeability in the clay may have also led to the higher degradation. Despite Chingola having lower bandgap energy as compared to South Luangwa, implying that it was absorbing more visible light than South Luangwa, its performance in the degradation of oil was still low, perhaps because South Luangwa had more favorable properties such as large surface area and pore volume.

#### Total organic carbon content analysis

The initial TOC content in the contaminated samples (control) was 35%. This value was used as a parameter to calculate the amount of oil that had been degraded and to choose the most suitable mitigation method from among landfarming, photochemical oxidation, and combined landfarming and photochemical oxidation. Fig. 5 displays the proportion of TOC still present in the soil using the Walkley-Black method (Emoyan *et al.*, 2018). A reduction in the TOC in all the treatments was observed (Fig. 5) with the highest reduction being in the biocarb + grafted south Luangwa (combined landfarming and photochemical oxidation method) with only 1.46% total carbon remaining after treatment, whereas the current landfarming method employed by MCM still had considerable TOC.

The control had the highest amount of total carbon residue (6.39%) under natural attenuation. The grafted South Luangwa/biocarb was better than the grafted Chingola/biocarb because the former had a higher surface area and greater pore volume, which enhanced the photocatalytic properties. The TOC reduction was a result of the reduction in the oil content. A similar trend in the TOC reduction was observed in relation to oil reduction.

#### *Kinetics of photochemical oxidation and landfarming*

Kinetics of photochemical oxidation and landfarming characterize the quantity or concentration of pollutant (oil) remaining in the soil at a specific time, making it possible to predict how much oil would still be available at a specific point in the future (Agarry et al., 2013). In the current study, the entire oil content data were fitted into the first-order kinetics (Akpoveta et al., 2011) using the equation  $C = C_0 e^{-kt}$ , where C represents the amount of oil contained in the soil milligram per kilogram (mg/kg) at a time t,  $C_0$  is the initial amount of oil contained in the soil (mg/kg), k is the degradation rate constant (/day), whereas t is the time in days and e is the base of natural log. Degradation rates and half-lives that were estimated by this model were compared to the treatment options used by Arjoon and Speight (2020). The degradation half-life ( $t_{1/2}$ ) = natural logarithm of 2 divided by K ( $\frac{\ln 2}{k}$ ) is the time taken for a substance to lose half of its amount and describes the contaminants' transformation (Agarry et al., 2013; Ofoegbu et al., 2015). Therefore, efficiencies of oil degradation for the treatment systems under study were done through kinetic modeling, which was used to determine the rates of chemical processes (Safdari et al., 2018). The concentrations of the oil left in the soil at regularly spaced intervals and their natural logarithms were plotted against time as shown (Fig. 6) to analyze the degradation processes. The first-order and second-order kinetics were both performed on the data, but the coefficient of determination ( $R^2$ ) values were higher for first order. The degradation followed first-order kinetics because the plots of the ln of oil concentration against time were linear (Shen et al., 2016; Wang et al., 2016).

The rate constants derived from first-order kinetic modeling in Fig. 6 show how different treatments affect oil breakdown in oil-contaminated soils relative to one another. Table 3 shows how each treatment affected the degradation rate constant (k) and the related

degradation half-lives ( $t_{1/2}$ ). The rate constant, k, was generally between 0.007 and 0.049/days, with 0.007/days being the rate constant for natural attenuation (control). The rate of degradation also increases with greater degradation rate constants, which leads to a decrease in the half-life of degradation (Agarry et al., 2013; Ofoegbu et al., 2015). The variations in the rate constants and half-life times observed in the different treatments may be due to a number of reasons including enhanced adsorption of contaminants and bioavailability in treatments where modified and grafted clay catalysts were combined with biocarb. The half-lives ranged from 15.2-94.8 days. When deciding whether or not to classify a chemical as persistent, the half-life might be utilized as the primary benchmark. Persistent substances exhibit a half-life that is longer than 40 days (Acharya et al., 2019; Mohajeri et al., 2013). Because different components of crude oil such as aliphatic, aromatic, and polycyclic chemicals have varying degradation rates, the prediction of oil degradation kinetics is frequently challenging and complex (Xu et al., 2015). The  $R^2$  values ranged from 0.848-0.93 (Table 3). The low  $R^2$  values obtained could be attributed to variations in temperature during the treatment period, given the study was conducted toward the end of the rainy season. Low  $R^2$  values ranging from 0.69-0.99 have been recorded in the past (Uba et al., 2019). Consequently, the  $R^2$  values found in this investigation show that the decline in oil concentrations in the soil as a function of time is linear and positively correlated (Nwankwegu et al., 2016).

The percentage variations in rate constants and half-lives between the different treatments are shown in Table 4. In this study, there was no significant difference in the rate of oil degradation or the amount of time needed for the oil to totally break down between the control and biocarb ( $p = 0.14$ ).

#### *ANOVA analysis*

The ANOVA test revealed that differences in treatment means were not statistically significant with  $p = 0.14$  as shown in Table 5. Multiple comparisons test showed that there was no significant difference between natural attenuation (control) and landfarming (biocarb), which is similar to the findings of Shen et al. (2016) where  $p = 0.912$ . There was a statistically significant difference between the control and biocarb + grafted South Luangwa ( $p = 0.029$ ) and biocarb and grafted South Luangwa ( $p = 0.037$ ). The oil decrease

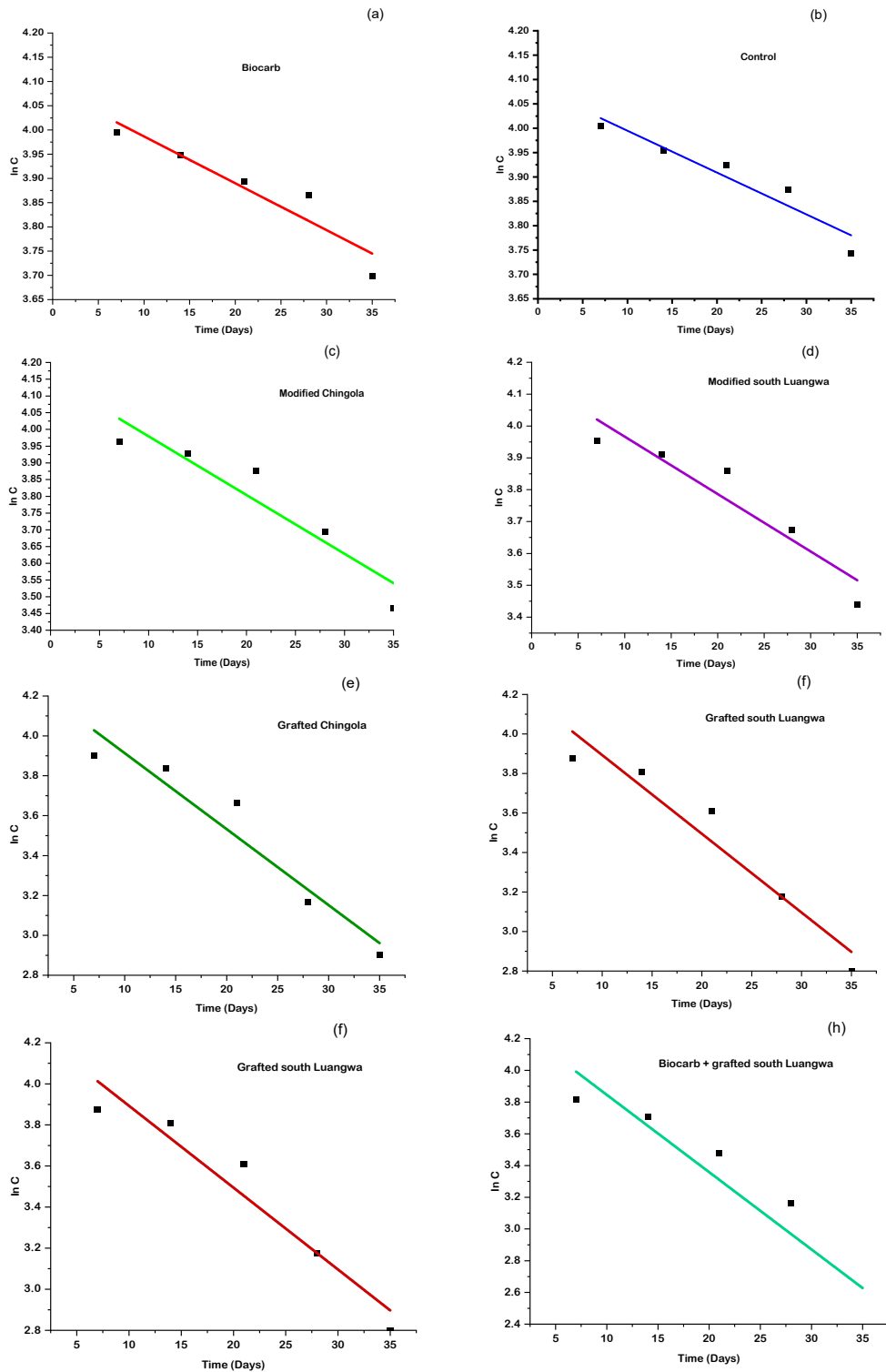


Fig. 6: First-order kinetics model fitted to the degradation data of oil in the soil treatments

Table 3: Relationship between treatment and rate of decay (half-life)

Sample	Control	Biocarb	MC	GC	ML	GL	B&GC	B&GL
Rate constant	0.007	0.008	0.018	0.038	0.015	0.040	0.046	0.049
Half-life (days)	94.802	83.094	44.971	30.130	39.487	18.194	17.395	15.201
$R^2$	0.871	0.859	0.907	0.924	0.848	0.931	0.894	0.881
$P$	0.004	0.005	0.006	0.003	0.006	0.003	0.005	0.005

MC (modified Chingola), GC (grafted Chingola), ML (modified South Luangwa), GL (grafted South Luangwa), B&GC (biocarb + grafted Chingola), B&GL (biocarb + grafted South Luangwa).

Table 4: Comparison of rate constants and half-lives for different treatments

Treatment	Difference in k (%)	Difference in $t_{1/2}$ (%)
Control and biocarb	13	13
Control and MC	72	71.3
Control and ML	88	82.4
Biocarb and MC	60.8	59.5
Biocarb and ML	76.9	71.15
Control and B&GC	78.8	74.79
Control and B&GL	80	77.7
MC and ML	11.76	8.47
Control and GC	74.69	58.86
Control and GL	75.86	73.73
Biocarb and GC	71.43	53.95
Biocarb and GL	66.67	70.39

in the control and biocarb + grafted Chingola was also significant ( $p = 0.043$ ). The quality of landfarming and photochemical oxidation were assessed from the percentage reduction of oil and TOC in the soil as seen from Figs. 4 and 5. The results are consistent with the study conducted by Fanaei et al. (2020). None of the treatments in photochemical oxidation, that is, modified MC, ML, GC, and GL, were significantly different from the control and biocarb treatments.

Oil degradation trends for each treatment are displayed in Fig. 7. The study has demonstrated that combined photochemical oxidation and landfarming (biocarb + GL and biocarb + GC) treatments of oil-contaminated soil can achieve high levels of oil removal, particularly for biocarb + GL, which also had the highest TOC removal as can be seen in Fig. 5 (Liao et al., 2018; Okonofua et al., 2020). The differences in degradation activity of biocarb + GL and biocarb + GC could be likely due to differences in the BET surface or density of  $\text{OH}^*$  present on their surfaces (Haque et al., 2012). For instance, the South Luangwa (bentonite) utilized in this investigation is made up of an octahedral arrangement of  $\text{AlO}_2$  between two sheets of  $\text{SiO}_2$ .

Owing to isomorphic substitutions of Mg ions ( $\text{Mg}^{2+}$ ) for aluminum ions ( $\text{Al}^{3+}$ ) in the octahedral layer and  $\text{Al}^{3+}$  for Si ions ( $\text{Si}^{4+}$ ) in the tetrahedral layer, bentonite has a negative charge. Exchangeable cations (such as sodium ions, potassium ions, and calcium ions [ $\text{Na}^+$ ,  $\text{K}^+$ ,  $\text{Ca}^{2+}$  respectively]) are present in the interlayer area to counteract this negative charge. These cations make it easy for bentonite to adsorb pollutants, and they can be, naturally or through ionic exchange, exchanged with other metal cations (Bananezhad et al., 2019). These naturally occurring or exchanged cations provide clays, such as bentonite (South Luangwa); their affinity for aromatic hydrocarbons, which make up 17-50 percent weight of crude oil (Speight, 2016); and they also accelerate changes. Additionally, ML has a higher surface area compared to MC (Mambwe et al., 2023). The other reason for the increased degradation rate could have been due to the ability of biocarb to promote microbial activity. The use of biocarb plus GC and GL incorporated adsorption, chemical oxidation, and bioremediation. The combination of adsorption, photochemical oxidation, and bioremediation is known to produce little to no residues and produces

Table 5: ANOVA statistical results

Oil content	ANOVA				
	Sum of squares	Df	Mean square	F	Sig.
Between groups	1720.795	7	245.828	1.688	.140
Within groups	5824.173	40	145.604		
Total	7544.968	47			

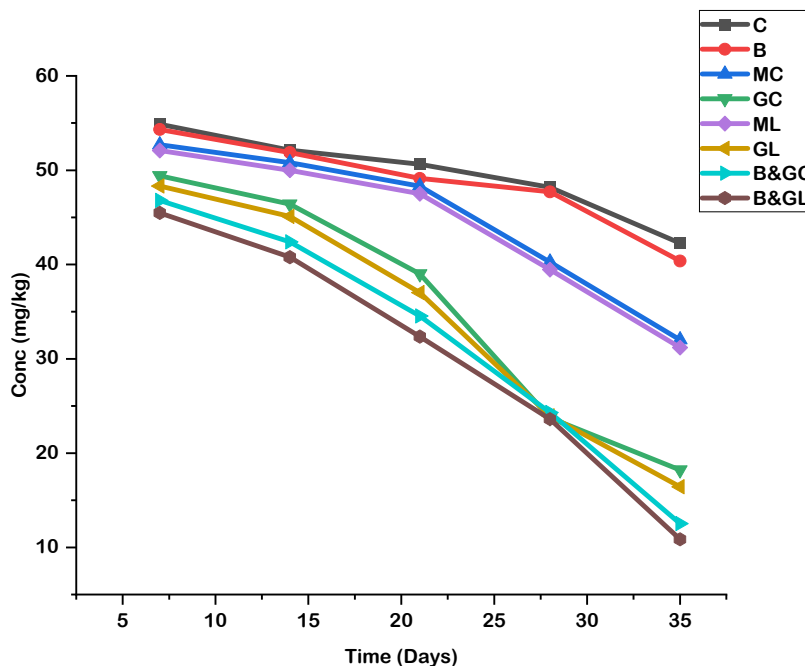


Fig. 7: Concentrations of oil in the various treatments from day 7-35. C (control), MC (modified Chingola), GC (grafted Chingola), ML (modified South Luangwa), GL (grafted South Luangwa), B and GC (biocarb + grafted Chingola), B and GL (biocarb + grafted South Luangwa)

a low carbon footprint, making it a cost-effective way to treat oils in all environmental media (Okoh *et al.*, 2020). Nonetheless, adding biocarb to the soil reduces soil density, thereby increasing porosity and the rate at which oxygen is distributed in the soil (Wang *et al.*, 2019). Photochemical oxidation has been utilized as an additional approach to reduce pollutants to manageable levels and obtain molecules that are readily biodegradable (Yan *et al.*, 2023). Photochemical oxidation can promote bioremediation by increasing contaminated substrate bioavailability and biodegradability, supplying oxygen, and occasionally releasing nutrients (Sutton *et al.*, 2014). This is achieved by accumulation of oil particles on the clay surface, resulting in their immobilization via ion-dipole interactions, coordination, or exchange mechanisms (Srinivasan, 2011). When clays modified with TiO<sub>2</sub>/Mn

are irradiated with light, e<sup>-</sup>-hole pairs are created that when in contact with air form O<sub>2</sub><sup>•</sup> and OH<sup>•</sup> radicals. These radicals have the ability to nonselectively mineralize a range of adsorbed organic compounds into benign byproducts such as carbon dioxide, water, and inorganic ions, either partially or fully (Gaur *et al.*, 2022). Metal loading on the clay surface further enhances the material's surface area and pore volume (Mishra *et al.*, 2018). This then increases the number of active surface sites. The increased surface area allows for more molecules to interact with the surface, thereby hastening the degradation of oil molecules (Surya *et al.*, 2018). The doping of the clays with Mn leads to structural distortions and changes in the chemical composition. These changes affect the electronic structure and, as a result, alter the optical response by reducing the bandgap (Denison *et al.*,

Table 6: Summary of some remediation techniques for treating soil polluted with oil

Procedure	Focus	Results	Sources
Bioremediation	Wheat bran and swine wastewater were used to remediate the contaminated soil.	A degradation efficiency of $68.27 \pm 0.71$ percent was attained after 40 days.	Zhang <i>et al.</i> , 2020
Landfarming	Hydrocarbon-polluted soil was cleaned up using land farming, phytoremediation, and chemical-biological techniques.	Following treatment using the landfarming technique, a degradation of over 90% of the initial levels of the PAH and TPH was observed.	Okonofua <i>et al.</i> , 2020
Photochemical oxidation	The study coupled landfarming with photochemical oxidation with $\text{TiO}_2$ as a photocatalyst to remediate soil contaminated by crude oil.	The greatest removal efficiencies, of 67% and 59%, were obtained from 0.5% and 2% of $\text{TiO}_2$ .	Effendi and Aminati, 2019
Bioremediation	Petroleum-contaminated soil was treated using aged waste from landfills.	Following 98 days of treatment, efficiency increased from 22.40% to 89.83%.	Liu <i>et al.</i> , 2018
Natural attenuation	Enhancing long-term groundwater contamination at locations where attenuation-based treatments are being used	The physical and chemical mechanisms that cause pollutant attenuation were to be monitored closely as part of the long-term monitoring approach.	Denham <i>et al.</i> , 2020
Photochemical oxidation	The comparative photodegradation activities of pentachlorophenol (PCP) and polychlorinated biphenyls using UV alone and $\text{TiO}_2$ -derived photocatalysts in methanol soil washing solution	The percentages of PCP removed after 120 minutes were 94%, 92%, and 57%.	Zhou <i>et al.</i> , 2014
Bioremediation	The petroleum in the contaminated soil was broken down using sawdust and rice straw.	After 5 months, the TPH removal percentages were 23.9%, 45.2%, and 27.5%, whereas the PAH removal percentages for the sawdust, rice straw, and control treatments were 66.3%, 30.3%, and 26.9%.	Huang <i>et al.</i> , 2019

2022). Previous research works have shown that nutrition supplementation promotes bioremediation by boosting microbial biomass (Denham *et al.*, 2020). It is also possible that nutrients from biocarb could have boosted the microbial biomass, resulting in increased oil degradation in the treatments with combined photochemical oxidation and landfarming. Photochemical oxidation may increase the degradability of contaminants, generally through the cleavage of large organic compounds into smaller ones (Medina *et al.*, 2018). A study conducted by Zhou *et*

*al.* (2014) showed that the photodegradation rate rises with pH; the mechanism underlying this stimulatory impact is that more  $\text{OH}^{\bullet}$  may be generated when the soil pH is greater. Numerous remediation studies have revealed that the ideal pH range for accelerated pollutant degradation is often between pH 6.5 and 8.5, with a pH of 7.8 being the most favorable in the majority of soils. Permeability, growth of microorganisms, dissolution of soil metals, and accessibility of nutrients are all influenced by pH (Okoh *et al.*, 2020). This could be another reason for higher degradation

rates in the combined treatments. Our findings are similar to results obtained by [da Rocha et al. \(2012\)](#). In this study, the modified as well as the grafted clays showed superior oil decomposition compared to biocarb in the remediation of oil-contaminated soil. Enhanced hydrophobicity promotes hydrophobic interaction between clay and the oil molecules, which in turn enhance both adsorption capacity and the photocatalytic degradation efficiency. Increased porosity in GL could have increased permeability, allowing for easy diffusion of nutrients and bacteria ([Zhu et al., 2020](#)). Oil biodegraders sourced from oil-polluted sites have shown limited adaptation with low degradation rates owing to the wide oil metabolism pathways ([Cui et al., 2023](#)). This could have affected the degradation of oil in the biocarb and the control treatments. Abiotic variables such as sorption and volatilization cause natural attenuation to happen in the control ([Uba et al., 2019](#)), yet [Franco et al. \(2014\)](#) considered volatilization as a negligibly opposing process. These techniques are usually conducted in simulative environments, but when conducted in the fields where the conditions may not always be ideal, the results might vary. In the current study, experiments were conducted outside, but in most studies, experiments are carried out in simulative environments, and this may have contributed to the variations ([Bakina et al., 2021](#)). The degradation of oil in soils is a highly complicated process that depends on a variety of elements such as the nature of oil, degree and length of pollution, and characteristics of the soil itself ([Polyak et al., 2020](#)). As such, the exact combination of photochemical oxidation and landfarming to effectively remove oil-contaminated soil cannot be determined.

Similar studies performed indicate that the success of the remediation of oil-contaminated soil and other organic pollutants depends on several factors highlighted in the discussion. [Table 6](#) shows some of the studies and their findings.

## CONCLUSION

The various treatments used in the bioremediation of oil-contaminated soil produced positive results, but with varying degrees of oil breakdown, as well as a decline in the acidic content of the oil in the contaminated soil. Lower percentage degradations could be attributed to short time of treatment (35 days) because heavy oils present in the soil take time to break

down. The decrease in the amount of oil, which was estimated by the change in oil in soil before and after remediation, is one of the main indicators determining the effectiveness of treatments. The longest half-life time of 94 days was recorded in the control treatment. This shows that oil in the polluted soil can be degraded naturally, but the process maybe very slow and would be effective over a very long period of time. The shortest half-life time of 15 days was recorded in the combined photochemical oxidation and landfarming (biocarb + GL). Findings from this study suggest that remediation of oil-contaminated soil with biocarb + GL led to quick elimination of oil. Therefore, the combination of photochemical oxidation and landfarming was effective and significantly boosted the degradation and loss of oil in the contaminated soils with high degradation constants and low half-lives. It is also worth noting that mere reliance on bioremediation of the oil contaminants in the soil could take a very long time for significant remediation to be achieved. The minimal oil depletion observed in the control and biocarb soil justifies this view. The combined remediation techniques used in this study offer a promising, better, cheaper, and more eco-friendly approach that, if adequately applied in oil-polluted soil, will lead to a harmless and nontoxic environment for both plant and animal well-being. The findings also suggest that the effective breakdown of oil and reduction of the remediation period might be achieved using photochemical oxidation with clay materials. Treatment of soil with photochemical oxidation is predicted to increase the oil bioavailability and the rate at which it is degraded in the soil. Photochemical oxidation was found to be a better remediation technique of oil-contaminated soil compared to the landfarming method. There is a need for MCM to consider adopting photochemical oxidation as a remediation technique in its treatment of oil-contaminated soil within the vicinity of its mines. Although photochemical oxidation can thoroughly remedy oil-contaminated soil with great efficacy, research on the nature of the intermediate compounds produced during remediation is scarce. More research on the subject matter is required to understand how these substances impact the environment.

## AUTHOR CONTRIBUTIONS

K. K. Kalebaila, the corresponding author, has contributed in supervising. M. Mambwe assisted in the

data analysis, interpreting the results, and preparing the manuscript. M. Mambwe prepared all the tables and figures and interpretation of the results. T. Johnson participated in the supervision, interpretation of the results, and manuscript preparation.

#### ACKNOWLEDGEMENT

The Copperbelt University Africa Centre of Excellence for Sustainable Mining and the Ministry of Technology and Science supported this project. Sincere appreciation also goes to MCM for providing the contaminated soil samples and the biocarb.

#### CONFLICT OF INTEREST

The authors declare that there is no conflict of interests regarding the publication of this manuscript. In addition, the ethical issues, including plagiarism, informed consent, misconduct, data fabrication and/or falsification, double publication and/or submission, and redundancy, have been completely observed by the authors.

#### OPEN ACCESS

©2024 The author(s). This article is licensed under a Creative Commons Attribution 4.0 International License, which permits use, sharing, adaptation, distribution, and reproduction in any medium or format, as long as you give appropriate credit to the original author(s) and the source, provide a link to the Creative Commons license, and indicate if changes were made. The images or other third-party material in this article are included in the article's Creative Commons license, unless indicated otherwise in a credit line to the material. If material is not included in the article's Creative Commons license and your intended use is not permitted by statutory regulation or exceeds the permitted use, you will need to obtain permission directly from the copyright holder. To view a copy of this license, visit: <http://creativecommons.org/licenses/by/4.0/>

#### PUBLISHER'S NOTE

GJESM Publisher remains neutral with regard to jurisdictional claims in published maps and institutional affiliations.

#### ABBREVIATIONS

% Percent

%R	Percentage of oil degradation after treatment
°C	Degree Celsius
Al	Aluminum
Al <sup>3+</sup>	Aluminum ion
Al <sub>2</sub> O <sub>3</sub>	Aluminum oxide
ANOVA	Analysis of variance
B	Biocarb
B&GC	Biocarb + grafted Chingola
B&GL	Biocarb + grafted South Luangwa
BET	Brunauer Emmett Teller
BJH	Barret-Joyner-Halenda
C	Control
Ca <sup>2+</sup>	Calcium ion
Ce	Concentration of oil at time, t
Conc.	Concentration
Co	Initial concentration of oil (time is zero)
cm <sup>3</sup> /g	Cubic centimeters per gram
/day	Per day
E	Base of natural log
Eq	Equation
eV	Electron volt
FTIR	Fourier transform infrared
G	Gram
GC	Grafted Chingola
GL	Grafted South Luangwa
ICP	Inductively coupled plasma
K <sup>+</sup>	Potassium ion
K	Rate constant
Kg	Kilogram
Ln	Natural logarithm
lnC	Natural logarithm of concentration
LSD	Fisher's least significant difference
M	Molar
MC	Modified Chingola
MCM	Mopani Copper Mines
Mg <sup>2+</sup>	Magnesium ion
m <sup>2</sup> /g	Square meters per gram
mg/Kg	Milligrams per kilogram
Min	Minutes
ML	Modified South Luangwa
MI	Milliliter
Mm	Millimeter
Mn	Manganese

$Mn(NO_3)_2$	Manganese (II) nitrate
$Na^+$	Sodium ion
Nm	Nanometer
$OH^\bullet$	Hydroxyl radical
P	A statistical measurement used to validate a hypothesis against observed data
PAHs	Polyaromatic hydrocarbons
pH	Potential of hydrogen
$R^2$	Coefficient of determination
Si	Silicon
$Si^{4+}$	Silicon ion
$SiO_2$	Silicon dioxide
SPSS	Statistical Package for Social Sciences
t	Time
TOC	Total organic carbon
TOG	Total oil grease
TPH	Total petroleum hydrocarbons
$TiO_2/Mn$	Titanium dioxide per manganese
$Ti(OPr_4)$	Titanium isopropoxide
USEPA	United States Environmental Protection Agency
UC	Unmodified Chingola
UL	Unmodified South Luangwa
UV-Vis	Ultraviolet-visible spectroscopy
v:v	Volume per volume
XRF	X-ray fluorescence

## REFERENCES

- Abioye, O.P.; Agamuthu, P.; Abdul Aziz, A.R., (2011). Phytotreatment of soil contaminated with used lubricating oil using Hibiscus cannabinus. *Biodegradation*, 23 (2): 277–286 (10 pages).
- Acharya, K.; Werner, D.; Dolfing, J.; Barycki, M.; Meynet, P.; Mrozik, W.; Komolafe, O.; Puzyn, T.; Davenport, R. J., (2019). A quantitative structure-biodegradation relationship (QSBR) approach to predict biodegradation rates of aromatic chemicals. *Water Res.*, 157: 181-190 (10 pages).
- Agarry, S.E.; Aremu, M.O.; Aworanti, O.A., (2013). Kinetic modelling and half-life study on enhanced soil bioremediation of bonny light crude oil amended with crop and animal-derived organic wastes. *J. Pet. Environ. Biotechnol.*, 4(2): 137-147 (11 pages).
- Aichner, B.; Bussian, B.; Lehnik-Habrink, P.; Hein, S., (2013). Levels and spatial distribution of persistent organic pollutants in the environment: a case study of German forest soils. *Environ. Sci. Technol.*, 47(22): 12703-12714 (12 pages).
- Akinwumiju, A.S.; Adelodun, A.A.; Ogundeji, S.E., (2020). Geospatial assessment of oil spill pollution in the Niger Delta of Nigeria: an evidence-based evaluation of causes and potential remedies. *Environ. Pollut.*, 267: 115545 (13 pages).
- Akpoveta, O.V.; Egharevba, F.; Medjor, O.W.; Osaro, K.I.; Enyemike, E.D., (2011). Microbial degradation and its kinetics on crude oil polluted soil. *Res. J. Chem. Sci.*, 1 (16): 8-14 (7 pages).
- Almutairi, M.S., (2022). Determination of total petroleum hydrocarbons (TPHs) in weathered oil contaminated soil. *Environ. Eng. Res.*, 27(5): 210324 (7 pages).
- Arjoon, K.; Speight, J.G., (2020). Chemical and physical analysis of a petroleum hydrocarbon contamination on a soil sample to determine its natural degradation feasibility. *Inventions*, 5(3): 43 (10 pages).
- Bakina, L.G.; Chugunova, M.V.; Polyak, Y.M.; Mayachkina, N.V.; Gerasimov, A.O., (2021). Bioaugmentation: possible scenarios due to application of bacterial preparations for remediation of oil-contaminated soil. *Environ. Geochem. Health*, 43(6): 2347-2356 (10 pages).
- Baloyi, J.; Ntho; Moma, J., (2018). A novel synthesis method of Al/Cr pillared clay and its application in the catalytic wet air oxidation of phenol. *Catal. Lett.*, 148: 3655- 3668 (14 pages).
- Bananezhad, B.; Islami, M.R.; Ghonchepour, E.; Mostafavi, H.; Tikdari, A.M.; Rafiei, H.R., (2019). Bentonite clay as an efficient substrate for the synthesis of the super stable and recoverable magnetic nanocomposite of palladium ( $Fe_3O_4$ /Bentonite-Pd). *Polyhedron*, 162: 192-200 (9 pages).
- Brame, J.A.; Hong, S.W.; Lee, J.; Lee, S.H.; Alvarez, P.J.J., (2013). Photocatalytic pretreatment with food grade  $TiO_2$  increases the bioavailability and bioremediation potential of weathered oil from the deepwater horizon oil spill in the Gulf of Mexico. *Chemosphere*, 90(8): 2315-2319 (5 pages).
- Brown, D.M.; Bonte, M.; Gill, R.; Dawick, J.; Boogaard, P.J., (2017). Heavy hydrocarbon fate and transport in the environment. *Q. J. Eng. Geol. Hydrogeol.*, 50: 333–346 (14 pages).
- Cui, J.Q.; He, Z. Q.; Ntakirutimana, S.; Liu, Z.H.; Li, B.Z.; Yuan, Y.J., (2023). Artificial mixed microbial system for polycyclic aromatic hydrocarbons degradation. *Front. Microbiol.*, 14 (1207196): (12 pages).
- da Rocha, O.R.S.; Dantas, R.F.; Duarte, M.M.B.; Duarte, M.M.L.; da Silva, V. L., (2012). Remediation of petroleum contaminated soil by photo-Fenton process applying black, white and germicidal light. *Afinidad*, 69 (557): 42-46 (5 pages).
- Denham, M.E.; Amidon, M.B.; Wainwright, M.; Dafflon, B.; Ajo-Franklin, J.; Eddy-Dilek, C.A., (2020). Improving long-term monitoring of contaminated groundwater at sites where attenuation based remedies are deployed. *Environ. Manage.*, 66: 1142-1161 (20 pages).
- Denison, S.B.; Da Silva, P.D.; Koester, C.P.; Alvarez, P.J.; Zygourakis, K., (2022). Clays play a catalytic role in pyrolytic treatment of crude-oil contaminated soils that is enhanced by ion-exchanged transition metals. *J. Hazard. Mater.*, 437: 129295 (9 pages).
- Dlamini, M.C.; Dlamini, M.L. Mente, P.; Tlhaole, B.; Erasmus, R.; Maubane-Nkadameng, M.S.; Moma, J.A., (2022). Photocatalytic abatement of phenol on amorphous  $TiO_2$ -BiOBr-bentonite heterostructures under visible light irradiation. *J. Ind. Eng. Chem.*, 111: 419-436 (18 pages).
- Dzionek, A.; Wojcieszynska, D.; Guzik, U., (2016). Natural carriers in bioremediation: a review. *Electron. J. Biotechnol.*, 23: 28–36 (9 pages).
- Effendi, A.J.; Aminati, T., (2019). Enhancing bioremediation of crude oil contaminated soil by combining with photocatalytic process using  $TiO_2$  as catalyst. *Geomate J.*, 17 (64): 100-107 (8 pages).
- Emoyan, O.O.; Akporido, S.O.; Agbaire, P.O., (2018). Effects of soil

- pH, total organic carbon and texture on fate of polycyclic aromatic hydrocarbons (PAHs) in soils. *Global NEST J.*, 20(2): 181-187 **(7 pages)**.
- Fanaei, F.; Moussavi, G.; Shekoochian, G., (2020). Enhanced treatment of the oil-contaminated soil using biosurfactant-assisted washing operation combined with H<sub>2</sub>O<sub>2</sub>-stimulated biotreatment of the effluent. *J. Environ. Manage.*, 271: 110941 **(8 pages)**.
- Farooq, S.; ASiddiq, A.; Ashraf, S.; Haider, S.; Imran, S.; Shahida, S.; Qaisar, S., (2022). Effective removal of arsenic (V) from aqueous solutions using efficient CuO/TiO<sub>2</sub> nanocomposite adsorbent. *Eur. J. Chem.*, 13 (3): 284-292 **(9 pages)**.
- Franco, M.G.; Corrêa, S.M.; Marques, M., Perez, D.V., (2014). Emission of volatile organic compounds and greenhouse gases from the anaerobic bioremediation of soils contaminated with diesel. *Water Air Soil Pollut.*, 225: 1-9 **(9 pages)**.
- Gaur, N.; Dutta, D.; Singh, A.; Dubey, R.; Kamboj, D.V., (2022). Recent advances in the elimination of persistent organic pollutants by photocatalysis. *Front. Environ. Sci.*, 10, 872514 **(29 pages)**.
- Gu, J.; Dong, D.; Kong, L.; Zheng, Y.; Li, X., (2012). Photocatalytic degradation of phenanthrene on soil surfaces in the presence of nanometer anatase TiO<sub>2</sub> under UV-light. *J. Environ. Sci.*, 24 (12): 2122-2126 **(5 pages)**.
- Hadei, M.; Mesdaghinia, A.; Nabizadeh, R.; Mahvi, A.H.; Rabbani, S.; Naddafi, K., (2021). A comprehensive systematic review of photocatalytic degradation of pesticides using nano TiO<sub>2</sub>. *Environ. Sci. Pollut. Res.*, 28: 13055-13071 **(18 pages)**.
- Hadnadjev-Kostic, M.; Vulic, T.; Marinkovic-Neducin, R., (2014). Solar light induced rhodamine B degradation assisted by TiO<sub>2</sub>-Zn-Al LDH based photocatalys. *Adv. Powder Technol.*, 25(5): 1624-1633 **(10 pages)**.
- Haque, M.M.; Detlef, B.; Mohammad, M., (2012). Photocatalytic degradation of organic pollutants: Mechanisms and kinetics. Organic pollutants ten years after the Stockholm Convention—Environmental and analytical update. London, UK: IntechOpen **(33 pages)**.
- He, X.; de la Cruz, A.A.; O'Shea, K.E.; Dionysiou, D.D., (2014). Kinetics and mechanisms of cylindrospermopsin destruction by sulfate radical-based advanced oxidation processes. *Water Res.*, 63: 168-178 **(11 pages)**.
- Hesnawi, R.M.; Mogadami, F.S., (2013). Bioremediation of Libyan crude oil-contaminated soil under mesophilic and thermophilic conditions. *Apcbee Procedia*. 5: 82-87 **(6 pages)**.
- Huang, Y.; Pan, H.; Wang, Q.; Ge, Y.; Liu, W.; Christie, P., (2019). Enrichment of soil microbial community in the bioremediation of a petroleum contaminated soil amended with rice straw or sawdust. *Chemosphere*. 224:265-271 **(7 pages)**.
- Hussain, M.; Akhter, P.; Iqbal, J.; Ali, Z.; Yang, W.; Shehzad, N.; Russo, N., (2017). VOCs photocatalytic abatement using nanostructured titania-silica catalysts. *J. Environ. Chem. Eng.*, 5(4): 3100-3107 **(8 pages)**.
- Idowu, O.; Semple, K.T.; Ramadass, T.; O'Connor, W.; Hansbro, P.; Thavamani, P., (2019). Beyond the obvious: environmental health implications of polar polycyclic aromatic hydrocarbons. *Environ. Int.*, 123: 543-557 **(15 pages)**.
- Imam, A., Suman, S.K., Ghosh, D.; Kanaujia, P.K., (2019). Analytical approaches used in monitoring the bioremediation of hydrocarbons in petroleum-contaminated soil and sludge. *Trends Anal. Chem.*, 118: 50-64 **(15 pages)**.
- Jha, P.; Biswas, A.K.; Lakaria, B.L.; Saha, R.; Singh, M.; Rao, A.S., (2014). Predicting total organic carbon content of soils from Walkley and Black analysis. *Commun. Soil Sci. Plant Anal.*, 45 (6): 713-725 **(23 pages)**.
- Kang, C.U.; Kim, D.H.; Khan, M.A.; Kumar, R.; Ji, S.E.; Choi, K.W.; Paeng, K.J.; Park, S.; Jeon, B.H., (2020). Pyrolytic remediation of crude oil-contaminated soil. *Sci. Total Environ.*, 713: 1-8 **(8 pages)**.
- Kebede, G.; Tafese, T.; Abda, E.M.; Kamaraj, M.; Assefa, F., (2021). Factors influencing the bacterial bioremediation of hydrocarbon contaminants in the soil: mechanisms and impacts. *J. Chem.*, 2021: 1-17 **(17 pages)**.
- Khudur, L.S.; Shahsavari, E.; Miranda, A.F.; Morrison, P.D.; Nugegoda, D.; Ball, A.S., (2015). Evaluating the efficacy of bioremediating a diesel-contaminated soil using ecotoxicological and bacterial community indices. *Environ. Sci. Pollut. Res.*, 22: 14809-14819 **(11 pages)**.
- Kong, F.X.; Sun, G.D.; Liu, Z.P., (2018). Degradation of polyaromatic hydrocarbons in soil mesocosms by microbial/plant bioaugmentation: performance and mechanism. *Chemosphere*. 198: 83-91 **(9 pages)**.
- Liao, X.Y.; Wu, Z.; Li, Y.; Luo, J.; Su, C., (2018). Enhanced degradation of polycyclic aromatic hydrocarbons by indigenous microbes combined with chemical oxidation. *Chemosphere*. 213: 551-558 **(8 pages)**.
- Lin, M.S.; Huang, C.Y.; Lin, Y.C.; Lin, S.L.; Hsiao, Y.H.; Tu, P.C.; Cheng, P.C.; Cheng, S.F., (2022). Green remediation technology for total petroleum hydrocarbon-contaminated soil. *Agronomy*. 12(11): 2759 **(12 pages)**.
- Liu, J.; Zhang, G., (2014). Recent advances in synthesis and applications of clay- based photocatalysts: A review. *Phys. Chem. Phys.*, 16(18): 8178-8192 **(15 pages)**.
- Liu, Q.; Li, Q.; Wang, N.; Liu, D.; Zan, L.; Chang, L.; Gou, X.; Wang, P., (2018). Bioremediation of Petroleum contaminated soil using aged refuse from landfills. *Waste Manage.*, 77: 576-585 **(10 pages)**.
- Mambwe, M.; Kalebaila, K.K.; Johnson, T.; Moma, J., (2023). Modification and characterization of selected Zambian clays for potential use as photocatalysts. *Eur. J. Chem.*, 14 (3): 362-369 **(8 pages)**.
- Medina, R.; David Gara, P.M.; Fernandez-Gonzalez, A.J.; Rosso, J.A.; Del Panno, M.T., (2018). Remediation of a soil chronically contaminated with hydrocarbons through persulfate oxidation and bioremediation. *Sci. Total Environ.*, 618: 518-530 **(13 pages)**.
- Mekkiyah, H.M.; Al-Hamadani, Y.A.J.; Abdulhameed, A.A.; Resheq, A.S.; Mohammed, Z.B., (2023). Effect of crude oil on the geotechnical properties of various soils and the developed remediation methods. *Appl. Sci.*, 13: 9103 **(16 pages)**.
- Michael-Igolima, U.; Abbey, S.J.; Ifebeuegu, A.O., (2022). A systematic review on the effectiveness of remediation methods for oil. *Environ. Adva.*, 9: 100319 **(21 pages)**.
- Mishra, A.; Mehta, A.; Basu, S., (2018). Clay supported TiO<sub>2</sub> nanoparticles for photocatalytic degradation of environmental pollutants: A review. *J. Environ. Chem. Eng.*, 6(5): 6088-6107 **(25 pages)**.
- Mohajeri, L.; Aziz, A.H.; Isa, M.H.; Zahed, M.A., (2013). Effect of remediation strategy on crude oil biodegradation kinetics and half-life times in shoreline sediment samples. *Int. J. Mar. Sci. Eng.*, 3 (2): 99-104 **(5 pages)**.
- Naem, U.; Qazi, M.A., (2020). Leading edges in bioremediation

- technologies for removal of petroleum hydrocarbons. *Environ. Sci. Pollut. Res.*, 27(22): 27370-27382 **(13 pages)**.
- Nwankwegu, A.S.; Onwosi, C.O.; Orji, M. U.; Anaukwu, C.G.; Okafor, U.C.; Azi, F.; Martins, P.E., (2016). Reclamation of DPK hydrocarbon polluted agricultural soil using a selected bulking agent. *J. Environ. Manage.*, 172, 136-142 **(7 pages)**.
- Ofoegbu, R.U.; Momoh, Y.O.; Nwaogazie, I.L., (2015). Bioremediation of crude oil contaminated soil using organic and inorganic fertilizers. *J. Pet. Environ. Biotechnol.*, 6(1): 1 **(6 pages)**.
- Okoh, E.; Yelebe, Z.R.; Oruabena, B.; Nelson, E.S.; Indiamawei, O.P., (2020). Clean up of crude oil contaminated soils: bioremediation option. *Int. J. Environ. Sci. Technol.* 17(2): 1185-1198 **(14 pages)**.
- Okonofua, E.S.; Babatola, O.J.; Ojuri, O.; Lasis, K.H., (2020). Determination of suitable TPH remediation approach via MANOVA and inferential statistics assessment. *Remediation*. 30 (3): 75-87 **(13 pages)**.
- Polyak, Y.; Bakina, L.; Mayachkina, N.; Polyak, M., (2020). The possible role of toxigenic fungi in ecotoxicity of two contrasting oil-contaminated soils—A field study. *Ecotoxicol. Environ. Saf.*, 202:110959 **(10 pages)**.
- Safdari, M.S.; Kariminia, H.R.; Rahmati, M.; Fazlollahi, F.; Polasko, A.; Mahendra, S.; Wilding, V.; Fletcher, T.H., (2018). Development of bioreactors for comparative study of natural attenuation, biostimulation, and bioaugmentation of petroleum-hydrocarbon contaminated soil. *J. Hazard. Mater.*, 342: 270-278 **(9 pages)**.
- Sakshi, S.S.K.; Haritash, A.K., (2019). Polycyclic aromatic hydrocarbons: soil pollution and remediation. *Int. J. Environ. Sci. Technol.*, 16: 6489-6512 **(23 pages)**.
- Sanie Jahromi, M.S.; Jahromi, S.; Sahraei, R.; Shafa, S.; Ghaedi, M.; Ranjbar, M.; Zabetiana, H., (2023) Comparison of Effects of Oral Melatonin and Gabapentin on Pain and Hemodynamic Symptoms in Patients Undergoing Upper Limb Orthopedic Surgery. *Eurasian J. Sci. Tech.*, 3(4): 165-173 **(9 pages)**.
- Samimi, M.; Shahriari Moghadam, M., (2020). Phenol biodegradation by bacterial strain O-CH1 isolated from seashore. *Global J. Environ. Sci. Manage.*, 6(1): 109-118 **(10 pages)**.
- Samimi, M.; Shahriari-Moghadam, M., (2021). Isolation and identification of *Delftia lacustris* Strain-MS3 as a novel and efficient adsorbent for lead biosorption: Kinetics and thermodynamic studies, optimization of operating variables. *Biochem. Eng. J.*, 173: 108091 **(9 pages)**.
- Samimi, M.; Mohammadzadeh, E.; Mohammadzadeh, A., (2023). Rate enhancement of plant growth using Ormus solution: optimization of operating factors by response surface methodology. *Int. J. Phytoremediation*, 25(12), 1636-1642 **(7 pages)**.
- Samimi, M.; Safari, M., (2022). TMU-24 (Zn-based MOF) as an advance and recyclable adsorbent for the efficient removal of eosin B: Characterization, equilibrium, and thermodynamic studies. *Environ. Prog. Sustain. Energy*, 41(5): e13859 **(9 pages)**.
- Saneha, S.; Pattamapitton, T.; Bualert, S.; Phewnil, O.; Wararam, W.; Semvimol, N.; Chunkao, K.; Tudsanaton, C.; Srichomphu, M.; Nachaiboon, U.; Wongsrikaew, O.; Wichittrakarn, P.; Chanthasoon, C., (2023). Relationship between bacteria and nitrogen dynamics in wastewater treatment oxidation ponds *Global J. Environ. Sci. Manage.*, 9(4): 707-718 **(12 pages)**.
- Sarkar, D.; Ferguson, M.; Datta, R.; Birnbaum, S., (2005). Bioremediation of petroleum hydrocarbons i n contaminated soils: comparison of biosolids addition, carbon supplementation, and monitored natural attenuation. *Environ. Pollut.*, 136(1): 187-195 **(9 pages)**.
- Schackow, A.; Correia, S.L.; Effting, C., (2020). Influence of microstructural and morphological properties of raw natural clays on the reactivity of clay brick wastes in a cementitious blend matrix. *Cerâmica*, 66: 154-163 **(10 pages)**.
- Shaker, Z.; Almkhtar, E., (2016). Bioaccumulation of petroleum hydrocarbons by *Melanopsis nodosa* (Gastropoda) in river Tigris within the city of Baghdad. *Iraq. Int. J. Curr. Microbiol. Appl. Sci.*, 5 (1): 244–251 **(8 pages)**.
- Sharifi, S., (2022) Oil Reservoirs and Exploitation of Oil Reservoirs. *Eurasian J. Sci. Tech.*, 2(2): 161-175 **(15 pages)**.
- Shen, W.; Zhu, N.; Cui, J.; Wang, H.; Dang, Z.; Wu, P.; Luo, Y.; Shi, C., (2016). Ecotoxicity monitoring and bioindicator screening of oil-contaminated soil during bioremediation. *Ecotoxicol. Environ. Saf.*, 124: 120-128 **(8 pages)**.
- Sihag, S.; Pathak, H.; Jaroli, D.P., (2014). Factors Affecting the Rate of Biodegradation of Polyaromatic Hydrocarbons. *Int. J. Pure Appl. Biosci.*, 2 (3): 185-202 **(18 pages)**.
- Silva-Castro, G.A.; Rodelas, B.; Perucha, C.; Laguna, J.; González-López, J.; Calvo, C., (2013). Bioremediation of diesel-polluted soil using biostimulation as post-treatment after oxidation with Fenton-like reagents: assays in a pilot plant. *Sci. Total Environ.*, 445: 347-355 **(9 pages)**.
- Soliman, R.M.; Sh El-Gendy, N.; Deriase, S.F.; Farahat, L.A.; Mohamed, A.S., (2014). The evaluation of different bioremediation processes for Egyptian oily sludge polluted soil on a microcosm level. *Energy Source. Part A.*, 36 (3): 231-241 **(11 pages)**.
- Speight, J.G., (2016). *Handbook of petroleum refining*. CRC press. 1st Edition. Boca Raton, USA, **(789 pages)**.
- Srinivasan, R., (2011). Advances in application of natural clay and its composites in removal of biological, organic, and inorganic contaminants from drinking water. *Adv. Mater. Sci. Eng.*, 2011: Article ID 872531 **(17 pages)**.
- Stepanova, A.Y.; Gladkov, E.A.; Osipova, E.S.; Gladkova, O.V.; Tereshonok, D.V., (2022). Bioremediation of soil from petroleum contamination. *Processes*. 10 (6): 1224 **(17 pages)**.
- Surya, L.; Sheilatina, P.V.P.; Sepia, N.S., (2018). Preparation and characterization of titania/bentonite composite application on the degradation of naphthol blue-black dye. *Res. J. Chem. Environ.*, 22(2): 48-53 **(6 pages)**.
- Sutton, N.B.; Grotenhuis, T.; Rijnaarts, H.H., (2014). Impact of organic carbon and nutrients mobilized during chemical oxidation on subsequent bioremediation of a diesel-contaminated soil. *Chemosphere*, 97: 64-70 **(7 pages)**.
- Sutton, N.B.; Maphosa, F.; Morillo, J., (2013). Impact of long-term diesel contamination on soil microbial community structure. *Appl. Environ. Microbiol.*, 79 (2): 619–630 **(12 pages)**.
- Thacharodi, A.; Hassan, S.; Singh, T.; Mandal, R.; Khan, H.A.; Hussain, M.A.; Pugazhendhi, A., (2023). Bioremediation of polycyclic aromatic hydrocarbons: An updated microbiological review. *Chemosphere*, 328:138498 **(20 pages)**.
- Uba, B.; Obidinma, M.; Chiamaka, A.; Obioma, C.O.; Chinazo, J.U., (2019). Kinetics of biodegradation of total petroleum hydrocarbon in diesel contaminated soil as mediated by organic and inorganic nutrients. *Anim. Res. Int.*, 16 (2): 3295 – 3307 **(13 pages)**.
- Ugochukwu, U.C.; Manning, D.A.; Fialips, C.I., (2014). Microbial degradation of crude oil hydrocarbons on organoclay minerals. J.

- Environ. Manage., 144: 197-202 (6 pages).
- Wang, S.Y.; Kuo, Y.C.; Hong, A.; Chang, Y.M.; Kao, C.M., (2016). Bioremediation of diesel and lubricant oil-contaminated soils using enhanced landfarming system. *Chemosphere*, 164: 558-567 (10 pages).
- Wang, C.C.; Li, J.R.; Lv, X.L.; Zhang, Y.Q.; Guo, G., (2014). Photocatalytic organic pollutants degradation in metal-organic frameworks. *Energy Environ. Sci.*, 7: 2831-2867 (37 pages).
- Wang, X.; Zheng, J.; Han, Z.; Chen, H., (2019). Bioremediation of crude oil-contaminated soil by hydrocarbon-degrading microorganisms immobilized on humic acid-modified biofuel ash. *J. Chem. Technol. Biotechnol.*, 94 (6): 1904-1912 (9 pages).
- Wu, M.; Ye, X.; Chen, K.; Li, W.; Yuan, J.; Jiang, X., (2017). Bacterial community shift and hydrocarbon transformation during bioremediation of short-term petroleum-contaminated soil. *Environ. Pollut.*, 223: 657-664 (9 pages).
- Xu, P.; Ma, W.; Han, H.; Jia, S.; Hou, B., (2015). Quantitative structure-biodegradability relationship for biokinetic parameter of polycyclic aromatic hydrocarbons. *J. Environ. Sci.*, 30: 180-185 (6 pages).
- Yan, X.; An, J.; Zhang, Y.; Wei, S.; He, W.; Zhou, Q., (2023). Photochemical degradation in natural attenuation of characteristics of petroleum hydrocarbons (C10-C40) in crude oil polluted soil by simulated long-term solar irradiation. *J. Hazard. Mater.*, 460: 132259 (10 pages).
- Yang, Y.; Javed, H.; Zhang, D.; Li, D.; Kamath, R.; McVey, K.; Alvarez, P.J., (2017). Merits and limitations of TiO<sub>2</sub>-based photocatalytic pretreatment of soils impacted by crude oil for expediting bioremediation. *Front. Chem. Sci. Eng.*, 11: 387-394 (8 pages).
- Yuniati, M.D., (2018). Bioremediation of petroleum-contaminated soil: A Review. *IOP conf. Series: Earth Environ. Sci.*, 118: 012063 (8 pages).
- Zhang, C.; Wu, D.; Ren, H., (2020). Bioremediation of oil contaminated soil using agricultural wastes via microbial consortium. *Sci. Rep.*, 10(1): 9188 (8 pages).
- Zhou, Z.; Zhang, Y.; Wang, H.; Chen, T.; Lu, W., (2014). The comparative photodegradation activities of pentachlorophenol (PCP) and polychlorinated biphenyls (PCBs) using UV alone and TiO<sub>2</sub>-derived photocatalysts in methanol soil washing solution. *PLoS One*, 9(9): e108765 (8 pages).
- Zhu, P.; Ren, Z.; Wang, R.; Duan, M.; Xie, L.; Xu, J.; Tian, Y., (2020). Preparation and visible photocatalytic dye degradation of Mn-TiO<sub>2</sub>/sepiolite photocatalysts. *Front. Mater. Sci.*, 14: 33-42 (10 pages).

#### AUTHOR (S) BIOSKETCHES

**Mambwe, M.**, Ph.D. Candidate, Department of Chemistry, School of Mathematics and Natural Sciences, Copperbelt University, Kitwe, Zambia.

- Email: [mambwemary@gmail.com](mailto:mambwemary@gmail.com)
- ORCID: 0000-0001-7181-822X
- Web of Science ResearcherID: JOZ-9585-2023
- Scopus Author ID: 57222756802
- Homepage: <http://www.researchgate.net/profile/Mary-Mambwe>

**Kalebaila, K.K.**, Ph.D., Instructor, Department of Chemistry, School of Mathematics and Natural Sciences, Copperbelt University, Kitwe, Zambia.

- Email: [kkalebai@gmail.com](mailto:kkalebai@gmail.com)
- ORCID: 0000-0003-3561-841X
- Web of Science ResearcherID: JNT-3646-2023
- Scopus Author ID: 57222761693
- Homepage: <https://www.cbu.ac.zm/schoolsAndUnits/schoolofmathematicsandnaturalsciences/dr-kalebaila-kabaso-kennedy/>

**Johnson, T.**, Ph.D., Instructor, Department of Biological Sciences, School of Mathematics and Natural Sciences, Copperbelt University, Kitwe, Zambia.

- Email: [tjforgood@gmail.com](mailto:tjforgood@gmail.com)
- ORCID: 0000-0001-6346-5604
- Web of Science ResearcherID: AAL-2618-2020
- Scopus Author ID: 57202336472
- Homepage: <https://www.cbu.ac.zm/schoolsAndUnits/schoolofmathematicsandnaturalsciences/dr-todd-johnson/>

#### HOW TO CITE THIS ARTICLE

Mambwe, M.; Kalebaila, K.K.; Johnson, T. (2024). Photochemical oxidation and landfarming as remediation techniques for oil-contaminated soil. *Global J. Environ. Sci. Manage.*, 10(2): 517-536.

DOI: 10.22035/gjesm.2024.02.07

URL: [https://www.gjesm.net/article\\_709756.html](https://www.gjesm.net/article_709756.html)

